# Radiometric Normalization of Multitemporal Optical Satellite Images using Iteratively-Reweighted Multivariate Alteration Detection


Bo-Yi Lin[1], Zhi-Jia Wang[2] and Chao-Hung Lin[3]

[1]National Cheng-Kung University, No.1, Daxue Rd., East Dist., Tainan, Taiwan
Email: pikadp2004@hotmail.com

[2]National Cheng-Kung University, No.1, Daxue Rd., East Dist., Tainan, Taiwan
Email: gj@dgl.xyz

[3]National Cheng-Kung University, No.1, Daxue Rd., East Dist., Tainan, Taiwan
Email: linhung@mail.ncku.edu.tw



**KEY WORDS:** radiometric normalization, PIF, MAD, GCCA, multitemporal satellite images



**ABSTRACT:** Radiometric normalization is a fundamental process for multitemporal satellite images. The accuracy of relative normalization depends on the quality of selected Pseudo Invariant Features (PIFs). PIFs represent the ground objects whose reflectance are constant during a period of time. In previous study, an algorithm, called Multivariate Alteration Detection (MAD), was applied to statistically select no-changed pixels within bi-temporal satellite images. However, MAD is sensitive to cloud covers and some clouds may be misclassified as PIFs. For this reason, Iteratively Reweighted MAD (IR-MAD) was introduced to establish an increasingly better no-changed background using iterative scheme. Nonetheless, both MAD and IR-MAD only compute the linear combinations for bi-temporal images, and not applicable for multitemporal images with more than two images. In this study, a novel method called Weighted Generalized Canonical Correlation Analysis (WGCCA) is proposed for the selection of high-quality PIFs in multitemporal and multispectral images, which solves coefficients for the correlations of not only multivariable data but also multitemporal data. Specifically, the proposed method integrates the strengths of Generalized Canonical Correlation Analysis (GCCA) and IR-MAD, and PIFs extraction from a sequence of satellite images is performed at the same time, which leads to a consistent feature extraction. Furthermore, when the high-quality PIFs are determined by the proposed method, the digital numbers of PIFs from multitemporal images are transformed into a predefined radiometric reference level. With this approach, the radiometric resolution of multitemporal images can be preserved, and a better radiometric normalization can be obtained. In experiment, SPOT-5 imagery was tested. Compared with Canonical Correlation Analysis (CCA) which is used in MAD, the proposed method can discriminate no-changed pixels from changed more precisely.


## 1. INTRODUCTION

With the development of satellite techniques, applications on remote-sensing images have attracted a lot of attentions. Especially, changes on earth surface within a certain period of time can be detected through high-resolution satellite images. However, change detection is influenced by different atmospheric conditions during multitemporal image acquisition. Therefore, radiometric normalization is a necessary pre-processing for many remote sensing change applications. Radiometric normalization is generally categorized into absolute and relative normalization. Absolute normalization converts the digital numbers of satellite images into the radiance of earth surface with the aids of sensor calibration data, atmospheric correction model and sun angle which are sometimes unavailable. In contrast, relative normalization converts the digital numbers of the target images into that of reference image without the requirement of additional data. However, the accuracy of relative normalization depends on the quality of selected Pseudo Invariant Features (PIFs)

Many approaches have been proposed for PIFs selection. Some approaches select landscape elements as PIFs even though the accuracy subjectively depends on visual inspection of landscape elements (Hall et al., 1991; Coppin et al., 1994). PIFs can be determined by Principal Component Analysis (PCA) with several constraints including Euclidean distance, spectral angle and spectrum correlation (Lin et al., 2014). Canty et al. (2002) utilized Multivariate Alteration Detection (MAD) to select PIFs for bi-temporal satellite images. MAD is invariant to linear and affine scaling while PCA is sensitive to the scale strength of variable. However, MAD does not work well in case that images contain many cloud covers because that mean value calculation on covariance matrix is affected by clouds. Therefore, the method called iteratively reweighted MAD (IR-MAD) was introduced to improve the shortcoming of MAD (Nielsen, 2007). IR-MAD applies weighted scheme to establish an increasingly better no-change background against which to detect change. Nonetheless, both MAD and IR-MAD are only feasible for bi-temporal images due to the basis of algorithms, that is, Canonical Correlation Analysis (CCA). To select PIFs from multi-temporal satellite images, Weighted Generalized Canonical Correlation Analysis (WGCCA) is proposed in this study to deal with multi-temporal images simultaneously while to discriminate no-changed pixels from changed more precisely, especially for cloud covers. As a result, a novel algorithm, called Multi-temporal and Multivariate Alteration Detection, is introduced to extract PIFs.

## 2. METHODOLOGY

In this study, PIFs in multitemporal satellite images are selected by the proposed WGCCA, which integrates the advantages of Iteratively Reweighted MAD and Generalized Canonical Correlation Analysis (GCCA). In this section, MAD, IR-MAD and GCCA will be briefly introduced in subsections 2.1-2.3, respectively, to clearly illustrate the proposed method. Then, the proposed method is presented in subsection 2.4.

### 2.1 Multivariate Alteration Detection

To select PIFs in bi-temporal images, the linear combinations of the intensities for *N* bands from bi-temporal images are constructed.

$$\begin{cases} \mathbf{U} = \mathbf{a}^{\mathrm{T}}\mathbf{X} = a_1X_1 + a_2X_2 + \cdots + a_{\mathrm{N}}X_{\mathrm{N}} \\ \mathbf{V} = \mathbf{b}^{\mathrm{T}}\mathbf{Y} = b_1Y_1 + b_2Y_2 + \cdots + b_{\mathrm{N}}Y_{\mathrm{N}} \end{cases} \tag{1}$$

where **X** and **Y** represent the random vectors of intensities for images acquired at time $t_1$ and $t_2$ respectively, and $(\mathbf{a}, \mathbf{b})$ are constant vectors. When the difference $(\mathbf{U} - \mathbf{V})$ is maximized, no-changed pixels are distinguished from changed ones, making PIFs to be easily detected. With this concept, Nielson et al. (1998) suggested that coefficients $(\mathbf{a}, \mathbf{b})$ are determined by CCA which leads to coupled generalized eigenvalue problems.

$$\begin{cases} {\mathbf{\Sigma}_{\mathrm{XX}}}^{-1}\mathbf{\Sigma}_{\mathrm{XY}}{\mathbf{\Sigma}_{\mathrm{YY}}}^{-1}\mathbf{\Sigma}_{\mathrm{YX}}\mathbf{a} = \rho^2\mathbf{a} \\ {\mathbf{\Sigma}_{\mathrm{YY}}}^{-1}\mathbf{\Sigma}_{\mathrm{YX}}{\mathbf{\Sigma}_{\mathrm{XX}}}^{-1}\mathbf{\Sigma}_{\mathrm{XY}}\mathbf{b} = \rho^2\mathbf{b} \end{cases} \tag{2}$$

where $\mathbf{\Sigma}_{XX}$ and $\mathbf{\Sigma}_{YY}$ are the covariance matrices of bi-temporal images while $\mathbf{\Sigma}_{XY}$ is inter-image covariance matrix.

However, MAD solved by CCA has two shortcomings. First, CCA is easily affected by a number of cloud cover changes in bi-temporal images due to that mean value in covariance matrix is disturbed by changed pixels. In other words, some clouds, regarded as non-PIFs, may be classified into PIFs. Second, there is no optimal NMAD threshold for the selection of high-quality PIFs.

### 2.2 Iteratively Reweighted MAD

To conquer the shortcomings of MAD, Nielson (2007) proposed an algorithm, called IR-MAD which employs a weighting scheme in MAD. The purpose of IR-MAD is to establish an increasingly better no-change background against which to detect change with the aids of giving high weights on pixels that exhibit little change over time while giving low weights on pixels that are more likely to be changed. Until the iteration meet termination criteria, optimal threshold for NMAD image can be found so that high-quality PIFs are eventually derived.

### 2.3 Generalized Canonical Correlation Analysis

Despite IR-MAD has already overcome the shortcomings of MAD solved by CCA, IR-MAD is still only feasible for computing linear combinations between bi-temporal images which is not applicable to long-term image series. For this reason, the proposed method attempts to solve MAD by GCCA instead of CCA. When MAD is solved by GCCA, MAD can deal with multi-temporal satellite images at the same time and the connections among images can be manually adjusted based on different applications. The objective functions of CCA (Eq. (3)) and GCCA (Eq. (4)) are almost the same, however GCCA aggregates the correlation coefficients of connected images by means of variable $C_{jk}$.

$$\text{Maximize:} \quad \boldsymbol{\rho}({\boldsymbol{\alpha}_{\mathrm{j}}}^{\mathrm{T}}\mathbf{x}_{\mathrm{j}}, {\boldsymbol{\alpha}_{\mathrm{k}}}^{\mathrm{T}}\mathbf{x}_{\mathrm{k}}) \tag{3}$$

$$\text{Maximize:} \quad \textstyle\sum_{j,k=1;j\neq k}^{N} C_{\mathrm{jk}}\boldsymbol{\rho}({\boldsymbol{\alpha}_{\mathrm{j}}}^{\mathrm{T}}\mathbf{x}_{\mathrm{j}}, {\boldsymbol{\alpha}_{\mathrm{k}}}^{\mathrm{T}}\mathbf{x}_{\mathrm{k}}) \tag{4}$$

$$\begin{cases} C_{\mathrm{jk}} = 1 & \text{if } \mathbf{x}_{\mathrm{j}} \text{ and } \mathbf{x}_{\mathrm{k}} \text{ are connected} \\ C_{\mathrm{jk}} = 0 & \text{otherwise} \end{cases},$$

where $(\mathbf{x}_{\mathrm{j}}, \mathbf{x}_{\mathrm{k}})$ are random vectors of reflectance for connected images while $(\boldsymbol{\alpha}_{\mathrm{j}}, \boldsymbol{\alpha}_{\mathrm{k}})$ are constant vectors. *N* means the number of images.

Unlike CCA, the coefficients $(\boldsymbol{\alpha}_1 \cdots \boldsymbol{\alpha}_{\mathrm{n}})$ of GCCA don't have analytical solution. In contrast, these coefficients $(\boldsymbol{\alpha}_1 \cdots \boldsymbol{\alpha}_{\mathrm{N}})$ are derived by iterated scheme which is similar to Wold's (1985) Partial Least Squares (PLS) algorithm (Figure 1). When the iteration meet a certain termination criteria (Eq. (6)), $(\boldsymbol{\alpha}_1 \cdots \boldsymbol{\alpha}_{\mathrm{n}})$ are then obtained.

$${\boldsymbol{\alpha}_{\mathrm{j}}}^{\mathrm{S}+1} = \left[\mathrm{Cov}\left(\mathbf{x}_{\mathrm{j}}, \mathbf{v}_{\mathrm{j}}^{\mathrm{S}}\right)^{\mathrm{T}}{\mathbf{\Sigma}_{\mathrm{jj}}}^{-1}\mathrm{Cov}\left(\mathbf{x}_{\mathrm{j}}, \mathbf{v}_{\mathrm{j}}^{\mathrm{S}}\right)\right]^{\frac{-1}{2}} * {\mathbf{\Sigma}_{\mathrm{jj}}}^{-1}\mathrm{Cov}(\mathbf{x}_{\mathrm{j}}, \mathbf{v}_{\mathrm{j}}^{\mathrm{S}}) \tag{5}$$

$$\mathbf{f}(\boldsymbol{\alpha}_1 \cdots \boldsymbol{\alpha}_N) = \sum_{j,k=1;j\neq k}^{N} C_{jk}\boldsymbol{\rho}\left(\boldsymbol{\alpha}_j{}^T\mathbf{x}_j, \boldsymbol{\alpha}_k{}^T\mathbf{x}_k\right) \\ \forall s \quad \mathbf{f}(\boldsymbol{\alpha}_1^S \cdots \boldsymbol{\alpha}_N^S) \leq \mathbf{f}(\boldsymbol{\alpha}_1^{S+1} \cdots \boldsymbol{\alpha}_N^{S+1}) \tag{6}$$

where $S$ represents the index of iteration while $\boldsymbol{v}_j$ is the inner component of $j^{\text{th}}$ image.

Nonetheless, PIFs selected by GCCA are almost the same as CCA since the weights on no-changed and changed pixels are the same. MAD solved by GCCA has two advantages compared to MAD solved by CCA. The first one is multi-temporal information can be taken into consideration during the computation of coefficients $(\boldsymbol{\alpha}_1 \cdots \boldsymbol{\alpha}_N)$. The other one is the coefficients can be obtained at the same time. Moreover, the amount of coefficients will be reduced. For instance, if there are $n$ images, the amount of coefficients in CCA will be $C_2^n$ (i.e.,$n!/2!\,(n-2)!$) while there are only $n$ coefficients in GCCA.

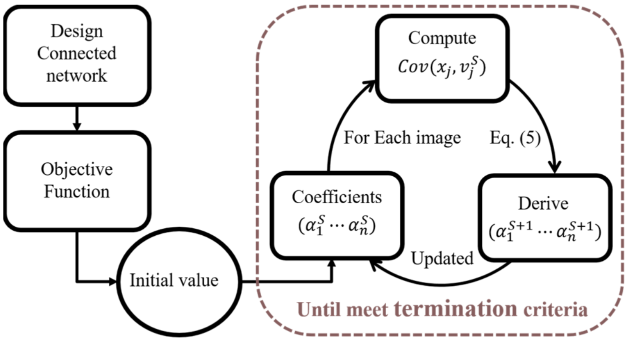


Figure 1. GCCA workflow. Coefficients of multi-temporal images can be found at the same time by means of GCCA algorithm.

### 2.4 Weighted Generalized Canonical Correlation Analysis

In fact, the quality of PIFs selected by GCCA for multi-temporal images is not good enough on account of misclassification on cloud covers. In this study, WGCCA is proposed to integrate the strengths of GCCA and IR-MAD, so that multi-temporal images can be processed simultaneously while high-quality PIFs will be separated from changed pixels more easily. The framework of WGCCA follows that of GCCA, as shown in Figure 2, however the weighting scheme in IR-MAD is also considered into the iteration of WGCCA.

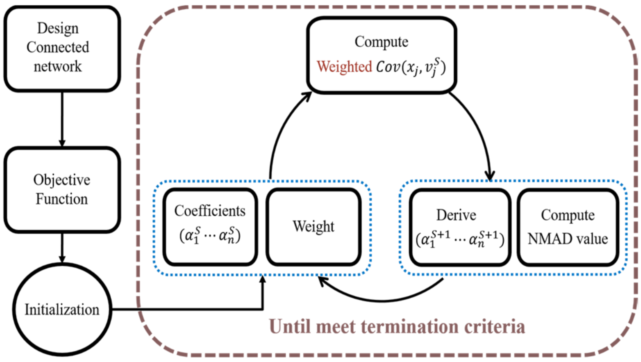


Figure 2. WGCCA workflow. High-quality PIFs for multi-temporal images are determined by integrating the strengths of GCCA and IR-MAD.

### 2.5 Design of Connected network

Theoretically, the target image can be connected with any others within the image series. In other words, the connected network can be designed in many ways based on different applications. In this study, the target image is attached to adjacent images in the input image sequence while the first and the last image are connected (Figure 3).

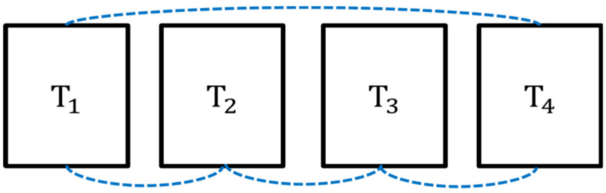

Figure 3. Connected network. Images are connected with adjacent images.

### 2.5.1 Objective function

According to the designed connected network, objective function is then constructed, which is the same as that of GCCA (Eq. (4)).

### 2.5.2 Iteration scheme

In WGCCA, there are two elements that should be initialized including coefficients and weight. Coefficients derived by CCA are regarded as initial values of coefficients $(\boldsymbol{\alpha}_1^0 \cdots \boldsymbol{\alpha}_N^0)$. Regarding weight for each pixel, spectral angle (Eq. (8)) is noticed for effectively discriminating no-change pixels from changed ones. Therefore, spectral angles of connected images are the initial values of inter-image weight $(weight_{jk})$ while initial value of weight $(weight_{jj})$ is obtained by taking the average of related $weight_{jk}$.

$$\text{Spectral angle: } \theta = \cos^{-1}\left(\frac{\mathbf{X}\cdot\mathbf{Y}}{\|\mathbf{X}\|\|\mathbf{Y}\|}\right) \tag{7}$$

where **X** and **Y** represents the random vectors of intensities for each pixel at time $t_1$ and $t_2$ respectively. The newer coefficients $(\boldsymbol{\alpha}_1^{S+1} \cdots \boldsymbol{\alpha}_N^{S+1})$ will be derived by means of Wcov $(\mathbf{x}_j, \mathbf{v}_j^S)$.

$$\boldsymbol{\alpha}_j^{S+1} = \left[ \mathrm{Wcov}(\mathbf{x}_j, \mathbf{v}_j^S)^T \boldsymbol{\Sigma}_{jj}^{-1} \mathrm{Wcov}(\mathbf{x}_j, \mathbf{v}_j^S) \right]^{\frac{-1}{2}} * \boldsymbol{\Sigma}_{jj}^{-1} \mathrm{Wcov}(\mathbf{x}_j, \mathbf{v}_j^S) \tag{8}$$

where $\mathrm{Wcov}(\mathbf{x}_j, \mathbf{v}_j^S) = C_{jk}\boldsymbol{\Sigma}_{jk}\boldsymbol{\alpha}_k^S$.

Because of the weighting scheme, each pixel from multitemporal images has its weight $w_i$. Thus, the mean value $\overline{X}$,covariance matrix $\boldsymbol{\Sigma}_{jk}$, and variance matrix $\boldsymbol{\Sigma}_{jj}$ are reformulated with weighting forms.

$$\begin{cases} \overline{X} = \sum_{i=1}^{n} w_i X_i \Big/ \sum_{i=1}^{n} w_i \\ \boldsymbol{\Sigma}_{jk} = \sum_{i=1}^{n} w_i (X_{ij} - \overline{X}_j)(X_{ik} - \overline{X}_k) \Big/ (n-1) \sum_{i=1}^{n} \frac{w_i}{n} \end{cases} \tag{9}$$

where $n$ is the total number of pixels.

Afterwards, NMAD images of the connected images are obtained through the newer coefficient $(\boldsymbol{\alpha}_1^{S+1} \cdots \boldsymbol{\alpha}_N^{S+1})$. If the NMAD value of a pixel is lower, this is more likely to be a PIF. In other words, the NMAD value is considered as new weight of a pixel due to the ability of distinguishing PIFs from changed pixels. Consequently, the new weight and coefficients will be used in Eq. (9). This process performed iteratively until meeting termination criteria.

## 3. EXPERIMENTAL RESULT

SPOT-5 images were utilized to evaluate the proposed method. SPOT-5 has four multispectral bands including green, red, NIR and SWIR band. The study area is located in Taiwan and the acquisition time are from 2003.05.31 to 2003.08.22.

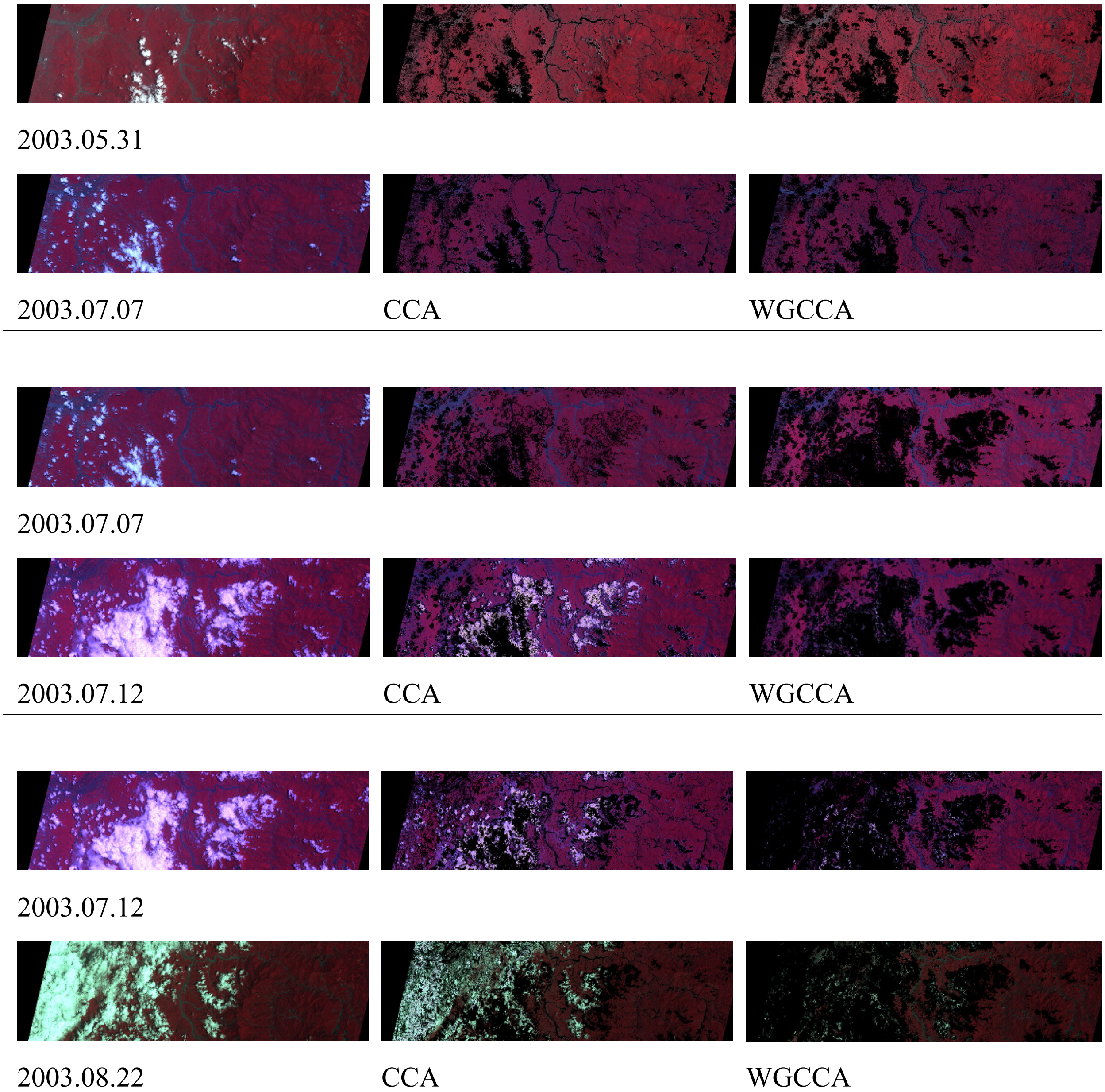


Figure 3. Comparison of PIFs selection methods based on CCA (Canty et al., 2004) and WGCCA. Left: three SPOT-5 tested bitemporal images (location: Taiwan); Middle: Results of CCA; Right: Results of WGCCA. PIFs and non-PIFs are displayed in pseudo color and black, respectively.

## 4. CONCLUSIONS

Previous studies on radiometric normalization selected PIFs based on MAD. However, MAD is sensitive to cloud covers and computes linear combinations only for bi-temporal images. In this study, a novel algorithm is proposed to integrate the strengths of GCCA and IR-MAD. The proposed method extracts PIFs from a sequence of satellite images simultaneously, which leads to a consistent feature extraction. Therefore, a novel method, called Multitemporal MAD, is introduced based on WGCCA. Further, Multitemporal MAD can extract high-quality PIFs, compared with MAD, which has been verified in the experiments. Although PIFs from WGCCA has higher quality than that from CCA, there are still some misclassifications in WGCCA including remaining clouds and water bodies which are generally considered to be non-PIFs. As a result, the weighting scheme in WGCCA will be reviewed in near future to obtain more reliable PIFs.

## 5. REFERENCES


Canty, M. J., Nielsen, A. A., & Schmidt, M., 2004. Automatic radiometric Normalization of Multitemporal Satellite Imagery. Remote Sensing of Environment, Vol. 91, pp. 441-451.

Canty, M. J., & Nielsen, A. A., 2008. Automatic Radiometric Normalization of Multitemporal Satellite Imagery with The Iteratively Re-weighted MAD transformation. Remote Sensing of Environment, Vol. 112, pp. 1025-2036.

Du, Y., Teillet, P. M., & Cihlar, J., 2002. Radiometric Normalization of Multitemporal High-resolution Satellite Images with Quality Control for Land Cover Change Detection. Remote sensing of Environment, Vol. 82, pp. 123-134.

Lin, C. H., Lin, B. Y., Lee, K. Y., & Chen, Y. C., 2015. Radiometric Normalization and Cloud Detection of Optical Satellite Images Using Invariant Pixels. ISPRS Journal of Photogrammetry and Remote Sensing, Vol. 106, pp. 107-117.

Marpu, P. R., Gamba, P., & Canty, M. J., 2011. Improving Change Detection Results of IR-MAD by Eliminating Strong Changes. IEEE Geoscience and Remote Sensing Letters, Vol. 8, No. 4, pp. 799-803.

Nielsen, A. A., 2007. The Regularized Iteratively Reweighted MAD Method for Change Detection in Multi-and Hyperspectral Data. IEEE Transactions on Image Processing, Vol. 16, No. 2, pp. 463-478.

Tenenhaus, A., & Tenenhaus, M., 2011. Regularized Generalized Canonical Correlation Analysis. Psychometrika, Vol. 76, No. 2, pp. 257-284.